catalysts

MDPI

Article

Selective Aerobic Oxidation of Benzyl Alcohol Driven by Visible Light on Gold Nanoparticles Supported on Hydrotalcite Modified by Nickel Ion

Dapeng Guo [1], Yan Wang [1,2], Peng Zhao [1], Meifen Bai [1], Hui Xin [1], Zhi Guo [1] and Jingyi Li [1,*]

[1] College of Chemistry and Chemical Engineering, Inner Mongolia University, Hohhot 010021, China; dapeng.105@163.com (D.G.); 15849381084@163.com (Y.W.); zp0476@126.com (P.Z.); bmf18247127121@163.com (M.B.); xinhui1128@163.com (H.X.); guozhi2256@163.com (Z.G.)

[2] Department of Chemical Engineering, Inner Mongolia Chemical Engineering Professional College, Hohhot 010070, China

* Correspondence: lijingyicn@163.com; Tel.: +86-138-4812-9221

Academic Editors: Stuart H. Taylor and Keith Hohn
Received: 28 November 2015; Accepted: 7 April 2016; Published: 27 April 2016

Abstract: A series of hydrotalcite (HT) and hydrotalcite modified by the transition metal ion Ni(II) was prepared with a modified coprecipitation method before being loaded with gold nanoparticles. The gold supported on Ni_3Al hydrotalcite with a Ni^{2+}/Al^{3+} molar ratio of 3:1 was investigated. Different techniques such as X-ray diffraction (XRD), X-ray photoelectron spectroscopy (XPS) and UV-vis diffuse reflection spectrum (UV-vis DRS) were applied to characterize the catalysts. A single-phase catalyst with high crystallinity, a layered structure and good composition was successfully fabricated. Good conversions and superior selectivities in the oxidation of benzyl alcohol and its derivatives were obtained with visible light due to the effect of localized surface plasmon resonance (LSPR) of gold nanoparticles and the synergy of the transition metal ion Ni(II). This reaction was proven to be photocatalytic by varying the intensity and wavelength of the visible light. The catalyst can be recycled three times. A corresponding photocatalytic mechanism of the oxidation reaction of benzyl alcohol was proposed.

Keywords: Ni(II) ion; hydrotalcite; Au nanoparticles; photo-oxidation; benzyl alcohol

1. Introduction

Selective oxidations of alcohols to carbonyl compounds, such as aldehydes and ketones, have been very important organic synthesis processes in academic research and industrial production [1]. The carbonyl compounds, such as aldehydes and ketones, were key intermediates in perfumes, spices, flame retardants, pharmaceuticals and other fine chemicals [2]. However, alcohols have been traditionally oxidized by a stoichiometric oxidant, such as dichromate and permanganate, and a large number of toxic and harmful byproducts were produced in the reaction [3]. In recent years, in the interest of green chemistry and environmental protection, oxygen application as an oxidant has caught the attention of researchers; in the process, pollution-free and clean water was the byproduct [4,5]. In addition, the selection of a green, pollution-free catalyst was also very important. The metal catalysts such as Ru [6,7], Pd [8,9], Rh [10,11], Cu [12,13], Pt [14,15], Au−Pd [16,17], Au−Cu [18] and Au−Ag [19] were commonly applied using oxygen as the oxidant in the oxidation of alcohols to aldehyde or ketone compounds. However, most of these were used in a homogeneous complex catalysis, in applications with high temperatures and high pressures requiring the addition of alkali, making the reaction conditions harsh. Thus, choosing recyclable and highly efficient catalysts in line with green chemistry and environmental protection policies became a major challenge for the field.

Hydrotalcite (HT) was a new type of clay layered with double-hydroxyl anionic material in the general chemical formula of $[M^{+2}{}_{1-x} \cdot M^{+3}{}_{x} \cdot (OH)_2]^{x+} \cdot [A^{n-}]_{x/n} \cdot yH_2O$. It had broad applications in catalysis, ion exchange, as well as flame retardant, medicinal, gene storage and other fields. According to the ferromagnetic property of M^{2+}, hydrotalcites were divided into ferromagnetic hydrotalcites and non-ferromagnetic hydrotalcites [20]. Currently, the use of MgAl hydrotalcite has been widely reported, whereas other types of hydrotalcite have their own useful characteristics. For example, the NiAl hydrotalcite has also had broad application in recent years. Choudary *et al.* initiated use of NiAl hydrotalcite as a catalyst by applying it in the selective oxidation of alcohols into ketones using oxygen. It can also be used as a precursor for new intercalated materials [21]. In this study, an Au catalyst was used with hydrotalcite as a carrier. Because of its double-hydroxyl layered structure, hydrotalcite can provide basic conditions for the reaction system and avoid the addition of extra alkaline substances in the reaction system [22]. Unlike traditional hydrotalcite, Mg^{2+} of MgAl hydrotalcite was transformed into Ni^{2+} in this study. If the Ni(II) ion species in the hydrotalcite can activate molecular oxygen, as suggested by Choudary *et al.*, Al(III) as a Lewis acid will assist in the reduction of dioxygen, consequently accelerating the alcohol oxidation reaction [21]. As a result of the pluralism of the transitional metal valence state, the electron transfer became so important that it can promote the electron transfer in the organic molecules, thus accelerating the reaction.

Until now, the heterogeneous catalytic oxidation of alcohols has been widely studied, but high temperature, high pressure and alkali conditions in the reaction still cannot be avoided. In this study, gold nanoparticles were supported on Ni_3Al HT (Au/Ni_3Al HT) and applied in the catalytic oxidation of benzyl alcohol. Due to the LSPR effect of gold nanoparticles [23], which allowed for the strong absorption of visible light, they can be stimulated by visible light. Better activities on Au/Ni_3Al HT by visible light and better recycling properties have occurred, compared with the results in other references [24–27]. The photocatalytic reaction can occur over Au supported on the hydrotalcite which can avoid the addition of alkaline substances. It can happen under normal temperature and atmospheric pressure. Therefore, it was a green and environmental friendly option.

2. Results and Discussion

2.1. Catalysts Characterization

2.1.1. X-ray Diffraction (XRD)

The structure and composition of the prepared samples have been studied by XRD. XRD with different supports are shown in Figure 1a. Peaks at 11.3, 22.7 and 34.5 degrees showed the support was a double-layer structure, and the growth of the crystal shape was satisfactory. With the increase of Ni(II) ion content, all the absorption peaks shifted to a smaller angular direction, due to the lattice expansion. A smaller peak at 32.3 degrees was the peak of $Al(OH)_3$ [28]. The gold catalysts on different hydrotalcite supports are shown in Figure 1b; the peaks were the same as that of the hydrotalcite supports. Some changes appeared in the characteristic peak of Au (111) at 38.2 degrees. Its peak intensity was stronger and the peak shape was even sharper than that in Figure 1a, a result of the appearance of gold nanoparticles and the larger size of the gold nanoparticles [24]. The layer frame of the hydrotalcite support was not damaged. The peaks of the catalysts with different gold loadings are shown in Figure 1c. With an increase in gold loading, the intensity of the characteristic peaks of Au (111) increased gradually, but the layer frame of the hydrotalcite support was not yet damaged. The particle size of Au or hydrotalcite of x wt. % Au/Ni_3Al HT (x = 0.5, 1, 2, 3, 4) was 2.33–2.35 nm.

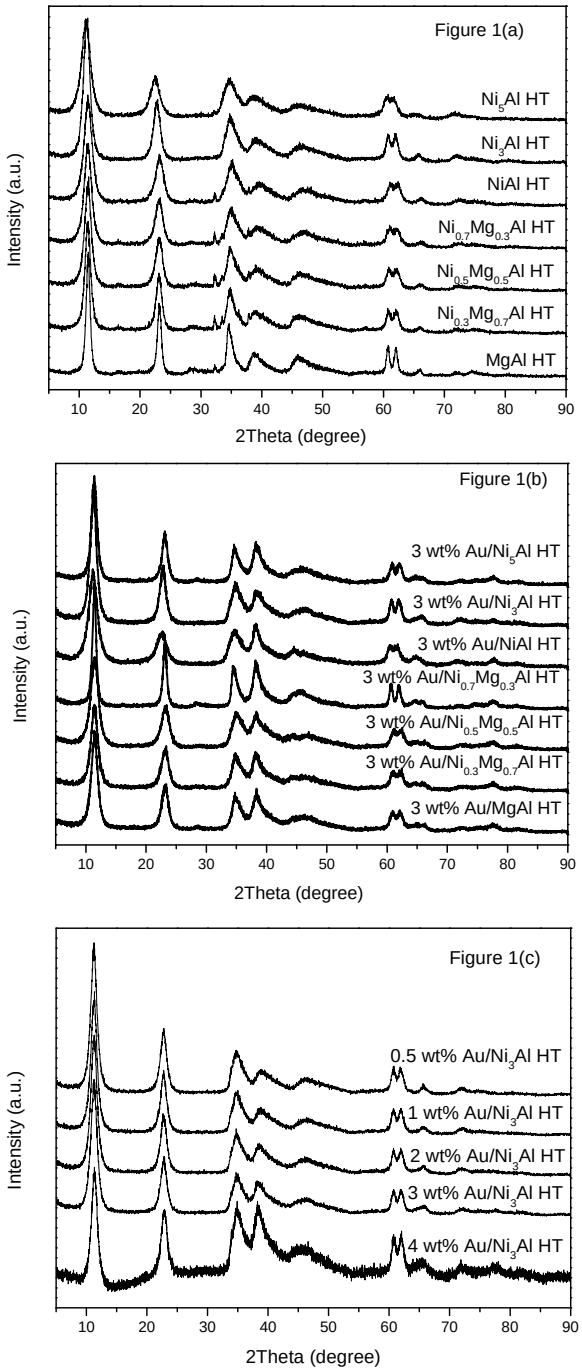

Figure 1. (**a**) XRD patterns of the different supports; (**b**) XRD patterns of the Au catalysts with various supports; (**c**) XRD patterns of the Au/Ni_3Al HT catalysts with different gold loadings.

2.1.2. X-ray Photoelectronic Spectra (XPS)

X-ray photoelectronic spectra (XPS) of the samples confirmed that gold existed in the metallic state on the HT. The corresponding Au 4f XPS spectrum for the 3 wt. % Au/Ni_3Al HT is shown in Figure 2a. As shown in Figure 2a, the binding energies for the Au $4f_{7/2}$ (83.70 eV) and Au $4f_{5/2}$ (87.35 eV) were observed which demonstrated the appearance of Au(0) [25,29]. The Ni 2p and the Al 2p XPS spectra for the 3 wt. % Au/Ni_3Al HT are shown in Figure 2b,c, and the appearance of Ni^{2+} and Al^{3+} can be proven by the results. Na 2s absorption peak appears in Figure 2c, because it was washed by sodium carbonate during the post-treatment.

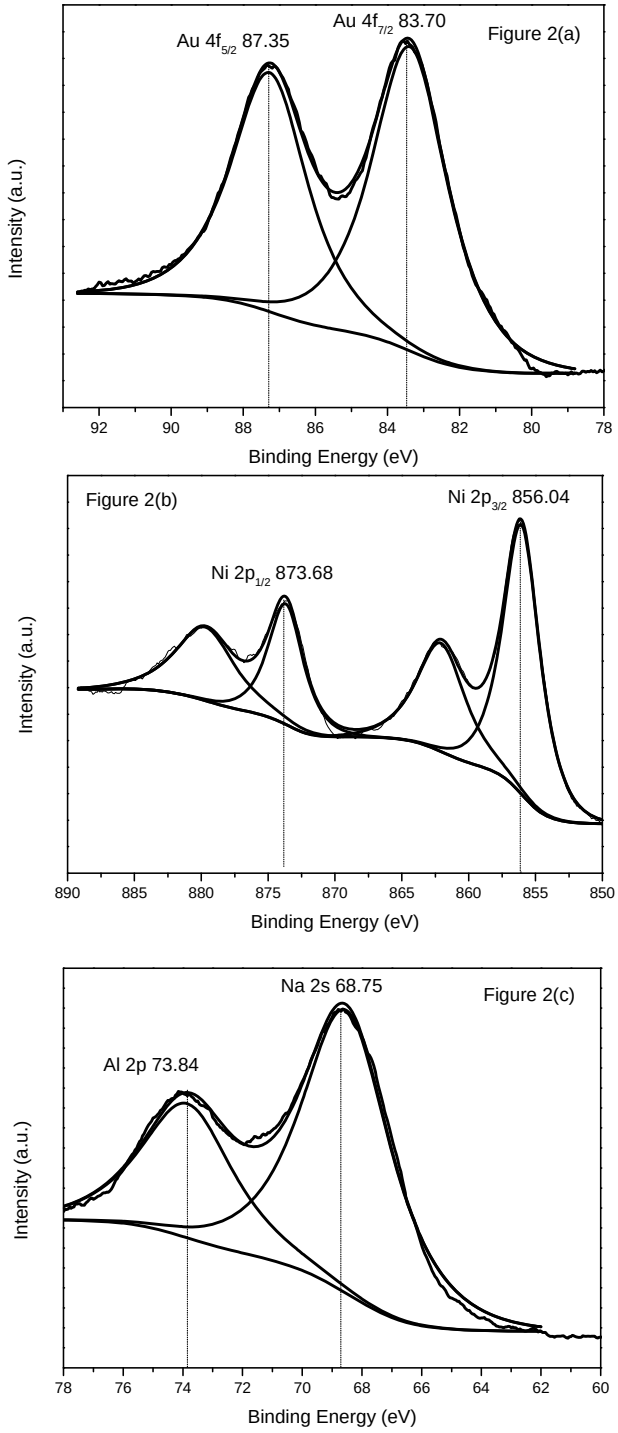

Figure 2. (**a**) XPS spectra of the Au 4f core level line for 3 wt. % Au/Ni_3Al HT; (**b**) XPS spectra of the Ni 2p core level line for 3 wt. % Au/Ni_3Al HT; (**c**) XPS spectra of the Al 2p core level line for 3 wt. % Au/Ni_3Al HT.

2.1.3. Ultraviolet-Visible Diffuse Reflectance Spectroscopy (UV-Vis DRS)

The UV-vis diffuse reflection spectra of MgAl HT, $Ni_xMg_{1-x}Al$ HT (x = 0.3, 0.5 and 0.7) and Ni_xAl HT (x = 1, 3 and 5) are demonstrated in Figure 3a. No absorption peaks appeared on the MgAl HT in the case of no gold in the wavelength range of visible light. Two obvious absorption peaks occurred on $Ni_xMg_{1-x}Al$ HT (x = 0.3, 0.5 and 0.7) and Ni_xAl HT (x = 1, 3 and 5) at approximately 380 nm and

640 nm. The peak at approximately 640 nm occurred because the nickel-modified hydrotalcite itself was green.

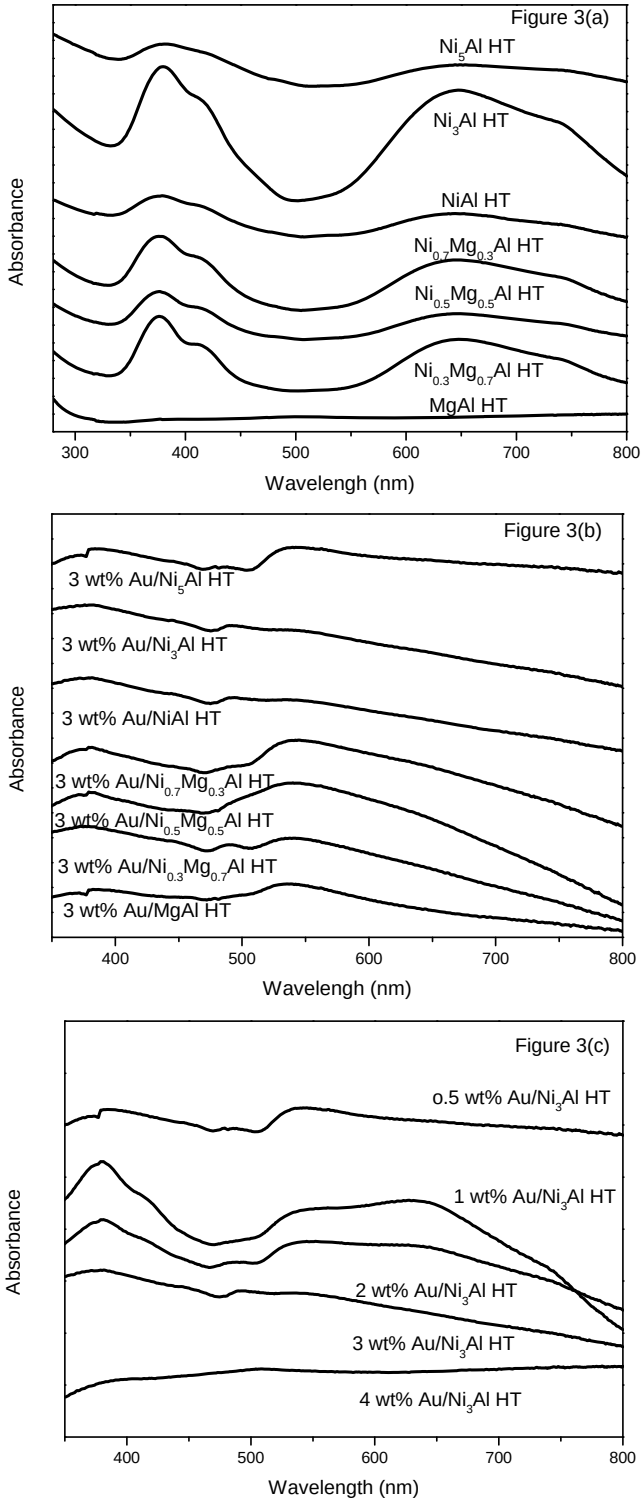

Figure 3. (**a**) UV-visible diffuse reflection spectra of the different supports; (**b**) UV-visible diffuse reflection spectra of the Au catalysts with various supports; (**c**) UV-visible diffuse reflection spectra of the Au/Ni_3Al HT catalysts with different gold loadings.

The UV-vis diffuse reflection spectra of Au/MgAl HT, Au/$Ni_xMg_{1-x}Al$ HT (x = 0.3, 0.5 and 0.7) and Au/Ni_xAl HT (x = 1, 3 and 5) are shown in Figure 3b. Compared with Figure 3a, the absorption peak at approximately 640 nm disappeared gradually. A strong absorption peak appeared at approximately 530 nm, consistent with the absorption of gold nanoparticles between 515 and 535 nm in the visible light range [30].

The UV-vis diffuse reflection spectra of the catalysts with different gold loadings are shown in Figure 3c. When the gold loading (wt. %) was 0.5% or 1%, three obvious absorption peaks appeared at approximately 380 nm, 530 nm and 640 nm, possibly caused by the lower gold loading which allowed for the display of the absorption peak of the hydrotalcite support and Au. When increasing the gold loading to 2%, 3% and 4%, the absorption peak at approximately 380 nm and 640 nm decreased gradually.

2.1.4. Atomic Absorption Spectroscopy (AAS)

The result of AAS of the 3 wt. % Au/Ni_3Al HT catalysts was analyzed in Table 1. The Ni^{2+} and Al^{3+} molar ratio was 3.3 on the hydrotalcite support; it was consistent with the theoretical mole ratio of 3 for Ni^{2+} and Al^{3+}. The gold content was 2.6 wt. %, which was consistent with the theoretical value (3 wt. %) of gold content. As seen from the results, the catalyst has been prepared successfully.

Table 1. Composition data obtained for 3 wt. % Au/Ni_3Al HT catalysts [a].

Sample	Chemical Composition (wt. %)			
	Ni^{2+}	Al^{3+}	Au	Ni^{2+}:Al^{3+} molar ratio
Au/Ni_3Al HT	40.5	5.8	2.6	3.3

[a] Determined by AAS.

2.2. Activity Test with Benzyl Alcohol

The conversion and selectivity of the oxidation of benzyl alcohol with different catalysts are summarized in Table 2. Benzyl alcohol was oxidized into benzaldehyde by using different catalysts. In Table 2's entries 1–7, poor light activities are shown on MgAl HT, $Ni_xMg_{1-x}Al$ HT (x = 0.3, 0.5 and 0.7) and Ni_xAl HT (x = 1, 3 and 5). In Table 2, entries 8–14, for the 3 wt % gold supported on MgAl HT, $Ni_xMg_{1-x}Al$ HT (x = 0.3, 0.5 and 0.7) and Ni_xAl HT (x = 1, 3 and 5), the activities of the catalysts appear enhanced compared with those of entries 1–7. The conversion of benzyl alcohol increased from 3 to 30 times. The conversion of benzyl alcohol was the highest of all the catalysts, with the greatest difference in the Au/Ni_3Al HT catalyst used in Table 2, entry 13. Table 2, entries 13 and 15–17, illustrate an increase in the gold loading as the oxidation activity of benzyl alcohol increased on Au/Ni_3Al HT. However, in Table 2, entry 18, the oxidation activity of benzyl alcohol decreased with 4 wt. % Au/Ni_3Al HT. The best catalytic activity occurred with 3 wt. % Au/Ni_3Al HT (Table 2, entry13).

Then, experiments were conducted to determine the best solvent. The oxidation of benzyl alcohol on 3 wt % Au/Ni_3Al HT in different solvents are shown in Table 3. In Table 3, entries 1–4, the conversion of benzyl alcohol to benzaldehyde was excellent in nonpolar solvents. When using benzotrifluoride as the solvent, the conversion occurred with the best result. In Table 3 entry 4, when using petroleum ether as the solvent, the selectivities for benzaldehyde decreased, and the other product was the corresponding benzyl benzoate [31]. As shown in Table 3 entries 5–8, the conversion of benzyl alcohol was lower in the other polar solvents except in ethanol. In Table 3, entry 8, when using methanol as the solvent, the selectivity for benzaldehyde has decreased, and the other product was the corresponding methyl benzoate. Because the hydroxyl group of methanol was activated, it would participate in this reaction quickly [31]. The results show that the conversion and selectivity of the oxidation of benzyl alcohol in benzotrifluoride was excellent.

Table 2. Oxidation of benzyl alcohol over the supported gold catalysts [a].

Entry	Catalyst	Conversion (%) [b]		Selectivity (%) [b]	
		Light	Dark	Light	Dark
1	MgAl HT	14.9	0.2	>99	>99
2	$Ni_{0.3}Mg_{0.7}Al$ HT	4.7	2.6	>99	>99
3	$Ni_{0.5}Mg_{0.5}Al$ HT	4.1	1.2	>99	>99
4	$Ni_{0.7}Mg_{0.3}Al$ HT	7.7	0.4	>99	>99
5	NiAl HT	1.4	0.3	>99	>99
6	Ni_3Al HT	6.5	4.5	>99	>99
7	Ni_5Al HT	5.6	4.5	>99	>99
8	Au/MgAl HT	31.2	5.0	>99	>99
9	$Au/Ni_{0.3}Mg_{0.7}Al$ HT	28.4	11.2	>99	>99
10	$Au/Ni_{0.5}Mg_{0.5}Al$ HT	31.4	1.2	>99	>99
11	$Au/Ni_{0.7}Mg_{0.3}Al$ HT	26.2	2.3	>99	>99
12	Au/NiAl HT	20.9	2.3	>99	>99
13	Au/Ni_3Al HT	41.1	6.8	>99	>99
14	Au/Ni_5Al HT	37.3	5.9	>99	>99
15	0.5 wt % Au/Ni_3Al HT	19.1	0.5	>99	>99
16	1 wt % Au/Ni_3Al HT	19.6	0.4	>99	>99
17	2 wt % Au/Ni_3Al HT	26.7	3.5	>99	>99
18	4 wt % Au/Ni_3Al HT	17.7	7.8	>99	>99

[a] Reaction conditions: 1, 4-dioxane (5 mL), benzyl alcohol (0.5 mmol), catalyst (50 mg), O_2 (1 atm), exposure time (24 h). Light source: 500 W halogen lamp. The solution temperature during exposure was 313 K; [b] Conversion rate and selectivity were determined by GC.

Table 3. Effect of the solvent on the aerobic oxidation of benzyl alcohol over 3 wt. % Au/Ni_3Al HT [a].

Entry	Solvent	Conversion (%) [b]		Selectivity (%) [b]	
		Light	Dark	Light	Dark
1	toluene	41.8	14.7	>99	>99
2	benzotrifluoride	74.5 (45.0) [c]	21.7 (3.9) [c]	>99	>99
3	1, 4-dioxane	68.6 (41.1) [c]	24.8 (6.8) [c]	>99	>99
4	petroleum ether	47.7	20.3	59.2 [d]	80.2 [d]
5	DMSO	5.9	1.8	>99	>99
6	DMF	23.6	11.6	>99	>99
7	ethanol	59.7	13.3	>99	>99
8	methanol	22.2	9.9	53.7 [e]	34.7 [e]

[a] Reaction conditions: solvent (5 mL), benzyl alcohol (0.5 mmol), catalyst (50 mg), O_2 (1 atm), exposure time (48 h). Light source: 500 W halogen lamp. The solution temperature during exposure was 313 K; [b] Conversion rate and selectivity were determined by GC; [c] Exposure time was 24 h; [d] The other product was benzyl benzoate; [e] The other product was methyl benzoate.

2.3. Oxidation of Various Alcohols

Through the selection of the catalyst and solvent, the optimal conditions for the oxidation of benzyl alcohol were 3 wt. % Au/Ni_3Al HT as the catalyst, benzotrifluoride as the solvent and oxygen as the oxidant with visible light irradiation.

Next, the conversion and selectivity of the oxidation of a broad range of alcohols with the proposed system are summarized in Table 4. The results of the oxidation of benzyl alcohol and its derivatives are shown in Table 4, entries 1–5. Excellent conversions and selectivities were found in all cases except with 4-nitro-benzyl alcohol [32]. Satisfactory conversions and selectivities were obtained in the oxidation of the other aromatic alcohols under the same conditions. Unfortunately, low conversion of the aliphatic alcohols can be found in Table 4, entries 8–9. Crotyl alcohol and *n*-octanol failed to be oxidized effectively resulting in less than 5% conversion of *n*-octanol. From these results, the oxidation of aliphatic alcohols proved to be unsatisfactory.

Table 4. Oxidation of different alcohols over 3 wt. % Au/Ni_3Al HT [a].

Entry	Substrate	Product	Conversion (%) [b]		Selectivity (%) [b]	
			Light	Dark	Light	Dark
1	benzyl alcohol	benzaldehyde	74.5	21.7	>99	>99
2	4-methyl benzyl alcohol	4-methyl benzaldehyde	60.1	27.2	>99	>99
3	4-methoxybenzylalcohol	4-methoxy benzaldehyde	77.8	34.4	>99	>99
4 [c]	4-nitro benzyl alcohol	4-nitrobenzaldehyde	21.4	5.1	>99	>99
5	4-chloro benzyl alcohol	4-chlorobenzaldehyde	62.7	18.8	>99	>99
6	phenylethanol	acetophenone	89.1	9.1	>99	>99
7	cinnamyl alcohol	cinnamyl aldehyde	67.7	5.8	>99	>99
8	crotyl alcohol	crotonaldehyde	32.1	17.0	>99	>99
9	*n*-octanol	*n*-octanal	4.8	0.3	>99	>99

[a] Reaction conditions: benzotrifluoride (5 mL), alcohol (0.5 mmol), catalyst (50 mg), O_2 (1 atm), exposure time (48 h). Light source: 500 W halogen lamp. The solution temperature during exposure was 313 K; [b] Conversion rate and selectivity were determined by GC; [c] Reaction solvent was 1, 4-dioxane.

2.4. Effect of Light Intensity and Light Wavelength

To prove that the reaction was driven by visible light, the experiments of light intensity and light wavelength have been performed. The results are shown in Figure 4. With an increase in the light intensity, the conversion of the oxidation of benzyl alcohol increased (Figure 4a). With a decrease in the wavelength range, the conversion of benzyl alcohol reduced gradually. In particular, when the wavelength was controlled between 550–800 nm and 600–800 nm, the conversion of the oxidation of benzyl alcohol decreased substantially (Figure 4b). The results were consistent with the strong absorption of gold nanoparticles between 515 and 535 nm (Figure 3) [30]. These experiments illustrated that the reaction was photocatalytic.

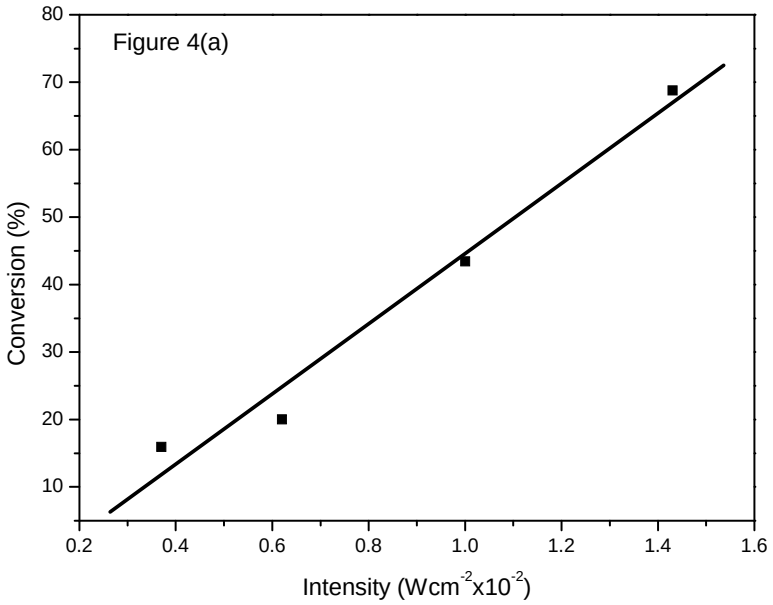

Figure 4. *Cont.*

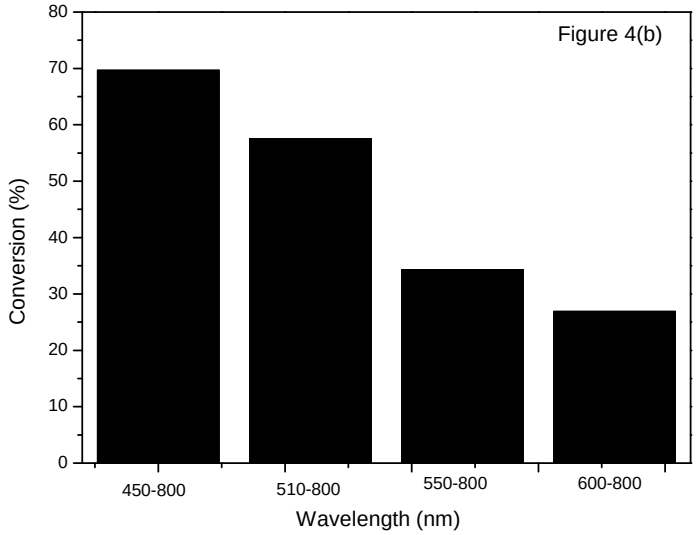

Figure 4. (**a**) Effect of light intensity on the photo-oxidation of benzyl alcohol; (**b**) Effect of the range of light wavelengths on the photo-oxidation of benzyl alcohol.

2.5. Reaction Mechanism

On the basis of the results from the experiments above, a plausible reaction mechanism is shown in Scheme 1. The mechanism illustrates that when the catalyst surface was irradiated by visible light, it can excite the gold nanoparticles on the surface of catalysts, making the activated gold nanoparticles adsorb the H atoms in the OH group of the benzyl alcohol and form Au−H [33]. Thus, the charge of each atom in the benzyl alcohol molecules has changed. The O atoms of the OH group in the benzyl alcohol molecules (with their negative charge) were adsorbed by the Al^{3+} of the hydrotalcite. At the same time, the Ni^{2+} adsorbed the dissociated O atoms from O_2 [21,26], which made the O atom adsorb the α-H of the benzyl alcohol. Then the α-H was fractured from the benzyl alcohol molecules, subsequently forming OH with the O atom on Ni^{2+}. The H atom adsorbed on the gold particles was fractured and combined with the OH adsorbed by Al^{3+} to form water. Next, the OH on the Ni^{2+} surface transferred to the surface of Al^{3+}, and the O atoms in the benzyl alcohol molecules adsorbed by Al^{3+} fell off, generating the final product benzaldehyde [28]. The catalyst can continue to participate in the reaction and complete the catalytic cycle.

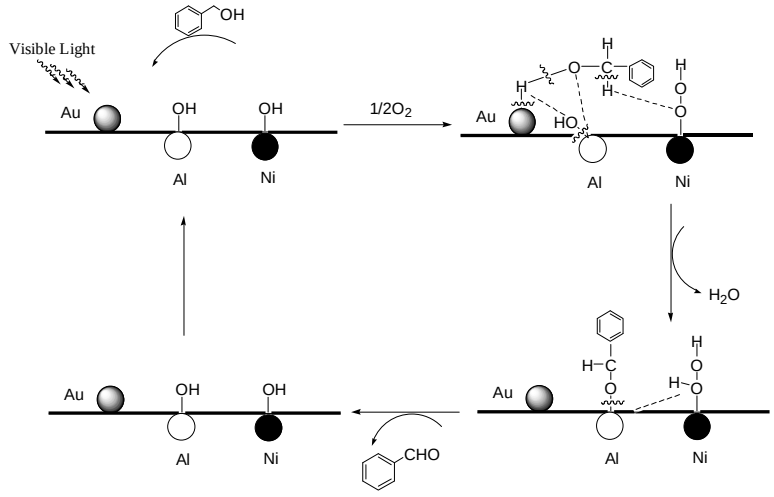

Scheme 1. The mechanism for the photocatalytic aerobic oxidations of benzyl alcohol using 3 wt. % Au/Ni_3Al HT.

The reaction mechanism over 3 wt. % Au/Ni_3Al HT was different from that over Au/MgAl HT [27] because oxygen took part in the reaction over Au/Ni_3Al HT at the beginning, whereas oxygen participated in the reaction after the production of benzaldehyde over Au/MgAl HT.

2.6. Recyclability Test

We tested the recyclability of the catalyst 3 wt. % Au/Ni_3Al HT by the conversion of the oxidation of the benzyl alcohol driven by visible light. In the first run, the conversion of the oxidation of the benzyl alcohol was 74.7%, and in the third run, the conversion of the oxidation of the benzyl alcohol was 67.3%. A minor fluctuation occurred during the conversion of the oxidation of the benzyl alcohol, its catalytic activity decreased slightly but the catalyst did not lose its activity. Therefore, the catalyst that we prepared can be reused.

3. Experimental Section

3.1. The Preparation of the Catalyst

3.1.1. The Preparation of the Hydrotalcite

The various hydrotalcite supports, Ni_xAl HT (x = 1, 3 and 5), were prepared by coprecipitation of $Ni(NO_3)_2 \cdot 6H_2O/AlCl_3 \cdot 6H_2O$ and $NaOH/Na_2CO_3$ solutions with a mechanical agitator by stirring at room temperature. They were then sedimented for 12 h at room temperature and washed five times in 0.1 mol$\cdot$ L^{-1} Na_2CO_3. Afterwards, they were dried at 80 °C for 20 h with a baking oven. Other hydrotalcite supports, such as MgAl HT (with $MgCl_2 \cdot 6H_2O$) and $Ni_xMg_{1-x}Al$ HT (x = 0.3, 0.5 and 0.7), were prepared with the same method [27,34]. Almost all reagents are purchased from J&K Technology Limited Company, Beijing, China. $NaBH_4$ (⩾98.0%, Sigma-Aldrich, St. Louis, MO, USA), $HAuCl_4 \cdot 3H_2O$ (⩾49.0% Au, Sigma-Aldrich, St. Louis, MO, USA), L-Lysine (⩾98.0%, J&K Technology Limited Company, Beijing, China). Benzyl alcohol (⩾99.0%, Sigma-Aldrich, St. Louis, MO, USA). Trifluorotoluene (⩾99.0%, J&K Technology Limited Company, Beijing, China).

3.1.2. The Preparation of Gold Nanoparticle Catalysts

A total of 3 wt. % Au/HT was supported by a $NaBH_4$ reduction method using $HAuCl_4 \cdot 3H_2O$ as the gold precursor and $NaBH_4$ as the reducing agent. The 3 wt. % Au/HT catalysts were prepared using a sequential deposition/reduction approach. HT (2.5 g) was dispersed in redistilled water (50 mL) and sonicated for 10 min. The pH value of the solution was adjusted to 10 using NaOH (0.5 mol$\cdot$ L^{-1}) with stirring. Next, the $HAuCl_4 \cdot 3H_2O$ solution was added dropwise under sonication. Subsequently, lysine (20 mL) was added to the mixture. After stirring for 30 min, a fresh $NaBH_4$ solution was added. This slurry was filtered before being washed with deionized water and ethanol, respectively. The resulting mixture was dried at 60 °C for 20 h. The catalysts of 3 wt. % Au/Ni_xAl HT (x = 1, 3 and 5, Au/Ni_xAl HT was the shortened form.), 3 wt. % $Au/Ni_xMg_{1-x}Al$ HT (x = 0.3, 0.5 and 0.7, $Au/Ni_xMg_{1-x}Al$ HT was the shortened form.), 3 wt. % Au/MgAl HT (Au/MgAl HT was the shortened form.), 0.5 wt. % Au/Ni_3Al HT, 1 wt. % Au/Ni_3Al HT, 2 wt. % Au/Ni_3Al HT and 4 wt. % Au/Ni_3Al HT were prepared with the same method [27,34].

3.2. Catalyst Characterization

The X-ray diffraction patterns (XRD) of the samples were recorded on a RIGAKU D/MAX-2500 (Rigaku Industrial Corporation, Osaka, Japan) X-ray diffractometer using CuKα radiation (λ = 1.5405 Å) at 40 kV and 100 mA. The diffraction data were collected from 5° to 80°. The X-ray photoelectron spectroscopy (XPS) measurements were performed on a Kratos XSAM800 (Kratos Company, Manchester, Britain) using AlKα radiation. The binding energy was calibrated using the C1s photoelectron peak at 284.8 eV as a reference. UV-visible diffuse reflectance spectra (UV-vis DRS) were detected on U-3900 made by Hitachi (Hitachi Limited Company, Tokyo, Japan). The gold contents of

the samples and the molar ratios of Ni and Al were quantitated using atomic absorption spectroscopy (AAS) on a GBC AVANTA YX-05 instrument (GBC Scientific Instrument Company, Melbourne, Australia). The product was quantitatively analyzed with a Shimadzu gas chromatograph-2014C (GC-2014C) (Shimadzu Company, Kyoto, Japan). The identity of the product was confirmed via gas chromatography-mass spectrometry (GC-MS) on a Finnigan LCQ Advantage MAX instrument (Finnigan Company, Silicon valley, CA, USA).

3.3. Selective Oxidation of Benzyl Alcohol

The reactions were carried out in a 50 mL round-bottom flask with a magnetic stirrer. In a typical run, a mixture of benzyl alcohol (0.5 mmol), trifluorotoluene (5 mL), the catalyst (50 mg; 3 wt. %) and oxygen as the oxidant was transferred into the reactor. Then, the solution was intensively stirred at 313 K and 1 atm for the reported time with a 500 W halogen lamp. Aluminized paper was wrapped around the flask, and the reaction was run under the light in order to try to make the dark reaction occur in the same external environment as the light reaction. The reactions were followed by gas chromatography (GC) and the structures of the products were confirmed by GC-MS (Finnigan Company, Silicon valley, CA, USA). The catalyst and reactants were separated via centrifugation. Afterward, to do the recycling experiment, the catalyst was washed with Na_2CO_3 (0.1 mol$\cdot$ L^{-1}) three times and ethanol once only. Finally, the catalyst was dried at 60 °C for 12 h. The recycled catalyst was reused in the next run under the same conditions.

4. Conclusions

In summary, it was demonstrated that the Ni-Al layered double hydroxides (LDHs) with a molar ratio of Ni^{2+} to Al^{3+} of 3 (Ni_3Al HT) can be used as a support for the photocatalytic oxidation of alcohols under base-free conditions with visible light irradiation under atmospheric pressure using O_2 as the sole oxidant. Through a series of characterization methods and experimental detections, the photocatalytic activity and selectivity were found to be excellent on 3 wt. % Au/Ni_3Al HT. A relatively reasonable mechanism was proposed. The oxidation of aromatic alcohols was superior using this catalyst, although the oxidation of aliphatic alcohols was not satisfactory—a topic that should become the focus of future research. In a word, Au supported on the hydrotalcite modified by the transition metal Ni was successfully applied to the oxidation of alcohols and it could be applied to other organic processes in the future.

Acknowledgments: This work was financially supported by the National Natural Science Foundation of China (NSFC, Nos. 20567002 and Nos. 21067007), the Education Department of Inner Mongolia Autonomous Region (NJ04093), Chunhui Plan of the Education Ministry (Z2004-2-15030 and Z2009-1-01005), the Natural Science Fund of Inner Mongolia (2010MS0203 and 2014MS0201), the 2013 Annual Grassland Talents Project of Inner Mongolia Autonomous Region and the 2013 Annual Inner Mongolia Talent Development Fund.

Author Contributions: D.G. carried out the catalyst preparation and their reaction activity studies and drafted the manuscript. Y.W., P.Z., M.B., H.X. and Z.G. participated in the design of the study and assisted in drafting the manuscript. All authors read and approved the final manuscript.

Conflicts of Interest: The authors declare no conflict of interest.

References

1. Dell'Anna, M.M.; Mali, M.; Mastrorilli, P.; Cotugno, P.; Monopoli, A. Oxidation of benzyl alcohols to aldehydes and ketones under air in water using a polymer supported palladium catalyst. *J. Mol. Catal. A* **2014**, *386*, 114–119. [CrossRef]
2. Sheldon, R.A.; Arends, I.W.C.E.; Dijksman, A. New developments in catalytic alcohol oxidations for fine chemicals synthesis. *Catal. Today* **2000**, *57*, 157–166. [CrossRef]
3. Tonucci, L.; Nicastro, M.; D'Alessandro, N.; Bressan, M.; D'Ambrosio, P.; Morvillo, A. Catalytic aerobic oxidation of allylic alcohols to carbonyl compounds under mild conditions. *Green Chem.* **2009**, *11*, 816–820. [CrossRef]

4. Punniyamurthy, T.; Velusamy, S.; Iqbal, J. Recent advances in transition metal catalyzed oxidation of organic substrates with molecular oxygen. *Chem. Rev.* **2005**, *105*, 2329–2364. [CrossRef]
5. Mallat, T.; Baiker, A. Oxidation of alcohols with molecular oxygen on solid catalysts. *Chem. Res.* **2004**, *104*, 3037–3058. [CrossRef]
6. Dijksman, A.; Marino-Gonzalez, A.; Payeras, A.M.; Arends, I.W.C.E.; Sheldon, R.A. Efficient and selective aerobic oxidation of alcohols into aldehydes and ketones using ruthenium/TEMPO as the catalytic system. *J. Am. Chem. Soc.* **2001**, *123*, 6826–6833. [CrossRef] [PubMed]
7. Csjernyik, G.; Ell, A.H.; Fadini, L.; Pugin, B.; Backvall, J.E. Efficient ruthenium-catalyzed aerobic oxidation of alcohols using a biomimetic coupled catalytic system. *J. Org. Chem.* **2002**, *67*, 1657–1662.
8. Liu, K.; Yan, X.J.; Zou, P.P.; Wang, Y.Y.; Dai, L.Y. Large size Pd NPs loaded on TiO_2 as efficient catalyst for the aerobic oxidation of alcohols to aldehydes. *Catal. Commun.* **2015**, *58*, 132–136.
9. Lien, C.H.; Medlin, J.W. Promotion of activity and selectivity by alkanethiol monolayers for Pd-catalyzed benzyl alcohol hydrodeoxygenation. *J. Phys. Chem. C* **2014**, *118*, 23783–23789.
10. Liu, L.H.; Yu, M.M.; Wayland, B.B.; Fu, X.F. Aerobic oxidation of alcohols catalyzed by rhodium(iii) porphyrin complexes in water: Reactivity and mechanistic studies. *Chem. Commun.* **2010**, *46*, 6353–6355. [CrossRef] [PubMed]
11. Tanaka, K.; Shoji, T.; Hirano, M. Cationic rhodium(I)/bisphosphane complex-catalyzed isomerization of secondary propargylic alcohols to α,β-enones. *Eur. J. Org. Chem.* **2007**, *2*, 2687–2699. [CrossRef]
12. Gamez, P.; Arends, I.W.; Reedijk, J.; Sheldon, R.A. Copper(II)-catalysed aerobic oxidation of primary alcohols to aldehydes. *Chem. Commun.* **2003**. [CrossRef]
13. Mitchell, L.J.; Moody, C.J. Solar photochemical oxidation of alcohols using catalytic hydroquinone and copper nanoparticles under oxygen: Oxidative cleavage of lignin models. *J. Org. Chem.* **2014**, *79*, 11091–11100. [CrossRef]
14. Li, Y.; Bian, T.; Du, J.S.; Xiong, Y.L.; Zhan, F.W.; Zhang, H.; Yang, D.R. Facile synthesis of high-quality Pt nanostructures with a controlled aspect ratio for methanol electro-oxidation. *Cryst. Eng. Commun.* **2014**, *16*, 8340–8343. [CrossRef]
15. Frassoldati, A.; Pinel, C.; Besson, M. Promoting effect of water for aliphatic primary and secondary alcohol oxidation over platinum catalysts in dioxane/aqueous solution media. *Catal. Today* **2011**, *173*, 81–88. [CrossRef]
16. Enache, D.I.; Edwards, J.K.; Landon, P.; Solsona-Espriu, B.; Carley, A.F.; Herzing, A.A.; Watanabe, M.; Kiely, C.J.; Knight, D.W.; Hutchings, G.J. Solvent-free oxidation of primary alcohols to aldehydes using Au-Pd/TiO_2 catalysts. *Science* **2006**, *311*, 362–365. [CrossRef] [PubMed]
17. Miedziak, P.; Sankar, M.; Dimitratos, N.; Lopez-Sanchez, J.A.; Carley, A.F.; Knight, D.W.; Taylor, S.H.; Kiely, C.J.; Hutchings, G.J. Oxidation of benzyl alcohol using supported gold–palladium nanoparticles. *Catal. Today* **2011**, *164*, 315–319. [CrossRef]
18. Sugano, Y.; Shiraishi, Y.; Tsukamoto, D.; Ichikawa, S.; Tanaka, S.; Hirai, T. Supported Au–Cu bimetallic alloy nanoparticles: An aerobic oxidation catalyst with regenerable activity by visible-light irradiation. *Angew. Chem.* **2013**, *125*, 5403–5407.
19. Huang, X.M.; Wang, X.G.; Wang, X.S.; Wang, X.X.; Tan, M.W.; Ding, W.Z.; Lu, X.G. P123-stabilized Au–Ag alloy nanoparticles for kinetics of aerobic oxidation of benzyl alcohol in aqueous solution. *J. Catal.* **2013**, *301*, 217–226.
20. Kovanda, F.; Jindová, E.; Lang, K.; Kubát, P.; Sedláková, Z. Preparation of layered double hydroxides intercalated with organic anions and their application in LDH/poly(butyl methacrylate) nanocomposites. *Appl. Clay Sci.* **2010**, *48*, 260–270.
21. Choudary, B.M.; Kantam, M.L.; Rahman, A.; Reddy, C.V.; Rao, K.K. The first example of activation of molecular oxygen by nickel in Ni-Al hydrotalcite: A novel protocol for the selective oxidation of alcohols. *Angew. Chem. Int. Ed.* **2001**, *40*, 763–766.
22. Debecker, D.P.; Gaigneaux, E.M.; Busca, G. Exploring, tuning, and exploiting the basicity of hydrotalcites for applications in heterogeneous catalysis. *Chem. Eur. J.* **2009**, *15*, 3920–3935. [CrossRef]
23. Zhu, H.Y.; Chen, X.; Zheng, Z.F.; Ke, X.B.; Jaatinen, E.; Zhao, J.C.; Guo, C.; Xie, T.F.; Wang, D.J. Mechanism of supported gold nanoparticles as photocatalysts under ultraviolet and visible light irradiation. *Chem. Commun.* **2009**. [CrossRef]

24. Feng, J.; Ma, C.; Miedziak, P.J.; Edwards, J.K.; Brett, G.L.; Li, D.; Du, Y.; Morgan, D.J.; Hutchings, G.J. Au-Pd nanoalloys supported on Mg-Al mixed metal oxides as a multifunctional catalyst for solvent-free oxidation of benzyl alcohol. *Dalton Trans.* **2013**, *42*, 14498–14508. [CrossRef]
25. Fang, W.H.; Chen, J.S.; Zhang, Q.H.; Deng, W.P.; Wang, Y. Hydrotalcite-supported gold catalyst for the oxidant-free dehydrogenation of benzyl alcohol: Studies on support and gold size effects. *Chem. Eur. J.* **2011**, *17*, 1247–1256. [CrossRef]
26. Kawabata, T.; Shinozuka, Y.; Ohishi, Y.; Shishido, T.; Takaki, K.; Takehira, K. Nickel containing Mg-Al hydrotalcite-type anionic clay catalyst for the oxidation of alcohols with molecular oxygen. *J. Mol. Catal. A* **2005**, *236*, 206–215.
27. Yu, J.; Li, J.Y.; Wei, H.L.; Zheng, J.W.; Su, H.Q.; Wang, X.J. Hydrotalcite-supported gold catalysts for a selective aerobic oxidation of benzyl alcohol driven by visible light. *J. Mol. Catal. A* **2014**, *395*, 128–136.
28. Wang, J.; Lang, X.J.; Zhaorigetu, B.; Jia, M.L.; Wang, J.; Guo, X.F.; Zhao, J.C. Aerobic oxidation of alcohols on Au nanocatalyst: Insight to the roles of the Ni–Al layered double hydroxides support. *ChemCatChem* **2014**, *6*, 1737–1747.
29. Kimura, K.; Naya, S.; Jin-Nouchi, Y.; Tada, H. TiO_2 crystal form-dependence of the Au/TiO_2 plasmon photocatalyst's activity. *J. Phys. Chem. C* **2012**, *116*, 7111–7117. [CrossRef]
30. Zhang, X.G.; Ke, X.B.; Zhu, H.Y. Zeolite-supported gold nanoparticles for selective photooxidation of aromatic alcohols under visible-light irradiation. *Chem. Eur. J.* **2012**, *18*, 8048–8056. [CrossRef]
31. Wei, H.L.; Li, J.Y.; Yu, J.; Zheng, J.W.; Su, H.Q.; Wang, X.J. Gold nanoparticles supported on metal oxides as catalysts for the direct oxidative esterification of alcohols under mild conditions. *Inorg. Chim. Acta* **2015**, *427*, 33–40. [CrossRef]
32. Heidarnezhad, A.; Zamani, F. Chromium containing Fe_3O_4/polyacrylonitrile–ethylenediamine as a magnetically recoverable catalyst for alcohol oxidation. *Catal. Commun.* **2015**, *60*, 105–109. [CrossRef]
33. Conte, M.; Miyamura, H.; Kobayashi, S.; Chechik, V. Spin trapping of Au-H intermediate in the alcohol oxidation by supported and unsupported gold catalysts. *J. Am. Chem. Soc.* **2009**, *131*, 7189–7196. [CrossRef] [PubMed]
34. Liu, P.; Li, C.; Hensen, E.J.M. Efficient tandem synthesis of methyl esters and imines by using versatile hydrotalcite-supported gold nanoparticles. *Chem. Eur. J.* **2012**, *18*, 12122–12129. [CrossRef] [PubMed]